Food Research 9 (Suppl. 1): 183 - 192 (2025)

Journal homepage: https://www.myfoodresearch.com



Automatic counting of *Paulownia* trees using unmanned aerial vehicle images and template matching technique

^{1,2,3,*}Khairunniza-Bejo, S., ²Baqir-Mahdi, W.M. and ⁴Nurhafizi-Zahari, M.

¹Institute of Plantation Studies, Universiti Putra Malaysia, 43400, Serdang, Selangor, Malaysia ²Department of Biological and Agricultural Engineering, Faculty of Engineering, Universiti Putra Malaysia, 43400 Serdang, Selangor Malaysia

³Smart Farming Technology Research Centre, Universiti Putra Malaysia, 43400 Serdang, Selangor Malaysia

⁴Green Afforestation International Network Sdn. Bhd., Revongen Corporation Centre Level 17, Top Glove Tower, No.16, Persiaran Setia Dagang Setia Alam, Seksyen U13 40170 Shah Alam, Selangor, Malaysia

Article history:

Received: 27 February 2024 Received in revised form: 26 November 2024 Accepted: 13 June 2025 Available Online: 17 July 2025

Keywords:

Template matching, Detection, Counting, Paulownia, Performance, Growing stages

DOI:

https://doi.org/10.26656/fr.2017.9(S1).127

Abstract

Paulownia has gained recognition as one of the swiftest-growing tree species globally and is used for medicinal, ornamental and timber purposes. The current conventional method of Paulownia tree counting is based on the ground manual survey which is timeconsuming. Therefore, the main objective of this study was to develop a suitable model for Paulownia tree counting using template matching and unmanned aerial vehicle imageries. First, the suitable template matching method was identified by comparing the performance of template matching with georeferencing data and template matching with the predetermined size of the template image. It was then followed by the development of an automatic Paulownia tree detection and counting model using the most suitable template matching technique at 4 different growing stages which are 3, 6, 9 and 12 months old. Results have shown that the template matching with georeferencing data performed better compared with the template matching with the predetermined size of the template image. For different growing stage models, the 3 and 6-month-old *Paulownia* tree models perform better compared to the others with an average F1-score of more than 85%. Results also revealed that younger Paulownia present greater homogeneity in crown morphology thus making it easier for the algorithm to detect Paulownia tree at younger age.

1. Introduction

Paulownia species are commonly grown in China and Japan due to their exceptional growth properties. For a minimum of 3000 years, China has been engaged in the cultivation of this plant (El-Showk and El-Showk, 2003) where historical records date back to the third century Before Christ (B.C.) for its medicinal, ornamental, and timber uses. Meanwhile, it has been cultivated in Japan for centuries and is highly valued in a variety of traditions. Although it is native to Northeast Asia, it has spread throughout the world as a result of naturalization. The Dutch East India Company introduced Paulownia to Europe during the 1830s, and it was subsequently brought to North America a few years thereafter. Paulownia has been acclimatized in the eastern United States for over 150 years and is also cultivated on the west coast. It can be concluded that Malaysia is pursuing

aggressively the planting of *Paulownia* (Latib *et al.*, 2020) in order to reduce the country's reliance on imported wood while also securing a consistent and environmentally responsible provision of timber materials. The demand for *Paulownia*-based products was one of the primary factors that influenced industrial players from all over the world to establish a *Paulownia* plantation in the first place.

Paulownia is a tree species that is experiencing rapid growth and expansion due to its short-rotation growth cycle. Under favourable environmental conditions, growth rates as high as 4 cm per year on an annual basis are conceivable (Koman et al., 2017). This implies that the cultivation of Paulownia trees in those nations is proving to be successful. Paulownia species grow exceptionally rapidly and can be harvested for good timber in as little as 15 years. Upon reaching five years

of age and being harvested, this tree yields a considerable amount of sawn timber that can be used for various purposes. Furthermore, when it reaches ten years of age, it has the potential to achieve an average diameter at breast height (DBH) of 35 cm. This diameter enables the production of sawn timber with a maximum volume of 0.5 m³. Therefore, it has garnered interest as a potential bioenergy crop capable of both carbon sequestration and transportation fuel production. Paulownia is a deciduous tree whose wood is renowned for its quality. Although it is lightweight and flexible, it is resistant to fracture and deformation and is highly regarded for its physical strength and texture, grain, and colour (Krikorian, 1988). The ring is crafted from acorns, a porous, straight-grained, and largely wood that is free from knots and has a smooth and glossy texture (Kaygin *et al.*, 2015).

Even though Paulownia is one of the most indemand products on the market, there are a few difficulties that the *Paulownia* grower frequently encounters when it comes to counting the trees to keep track of their progress. Tree counting is important because young Paulownia trees are extremely susceptible to a wide range of pests and diseases during this period of growth. Infection by witches' broom is the most common cause of death. Aside from that, it is primarily attacked by leaf-eating insects and borers, such as longhorn beetles, which feed on the leaves. In addition, scale insects and woodpeckers can be found in large numbers (Krikorian, 1988). Pest identification that is made too late after a pest attack could cause catastrophic damage to a farm's plantation and its products on the market. Following that, the importance of tree counting for monitoring the growth rate of the Paulownia tree cannot be overstated. The data collected from the Paulownia tree counting can be used to obtain information about tree growth, such as by analyzing the difference in height between the trees in the study area. Typically, tree counting is performed manually by a human. Instead of counting every single tree, some of the approaches just count the trees within a limited geographical zone (sampling region) and multiply the result by the plantation's total area. This process is timeconsuming, prone to errors, and requires a large number of workers. While significant progress has been made, certain issues remain with the tree-counting methods employed. One such concern is that some of these methods were tailored for specific geographical areas and may not be suitable for broader application in diverse large-scale scenarios (Maillard and Gomes, 2016; Wang et al., 2018; Xie et al., 2018). Different type of trees needs different algorithms for tree detection. This is because different tree canopies vary significantly in terms of colour, shape, and size, posing a challenge to

precisely classify trees. Furthermore, numerous of these methods aimed to establish distinct boundaries between various canopies, unnecessarily complicating the issues at hand (Pouliot *et al.*, 2002; Wagner *et al.*, 2018).

In the case of *Paulownia* trees, the existing methodology for tree counting has primarily relied on manual methods due to the challenges posed by overlapping canopies. Unlike certain agricultural products such as oil palm and rubber, for which template matching has shown promising results (Zainuddin and Daliman, 2020), the applicability of template matching techniques to *Paulownia* trees remains unexplored. Notably, template matching techniques excel when there exists a pronounced contrast between the target object, in this instance the *Paulownia* trees, and the background.

Template matching's effectiveness hinges on the presence of well-defined edges and clear separation of objects from the background. These factors influence its accuracy, and studies have shown that factors like image orientation, rotation, and template dimensions have a substantial impact on the performance of template-matching techniques (Kertész et al., 2015). Moreover, previous research has demonstrated the successful utilization of template matching for tree counting in various contexts, such as oil palm and rubber (Pollock, 1996; Larsen and Rudemo, 1998; Quackenbush et al., 2000; Olofsson et al., 2006; Larsen et al., 2011; Hung et al., 2012; Gomes and Maillard, 2013; Maillard and Gomes, 2016; Vahidi et al., 2018).

Given the distinct characteristics of *Paulownia* trees, their unique canopy arrangement, and the potential lack of clear boundaries between individual trees, it becomes crucial to investigate how template-matching methods can be adapted to this context. Hence, the present study aims to address this gap by exploring the viability of employing template matching for accurate tree counting in Paulownia groves. By considering factors such as image orientation, rotation, and template size, the study seeks to develop an approach that enhances the accuracy of tree counting, even in scenarios where canopies overlap. The findings of this research could provide valuable insights into automating the tree counting process for *Paulownia* trees, which has previously relied on manual efforts due to the challenges posed by their growth patterns and canopy structures.

2. Materials and methods

2.1 Study area and data collection

The study areas were located at various locations. For 3-month-old trees, it was located at Bahau plantation (2°45'44.34" N, 102°30'56.41" E, while for 6- and 9-month-old trees, it was located at Kundor plantation (2°

33'54.13" N, 102°00'42.08" E) and for 12-month-old trees, it was located at Rawang plantation (3°22'16.71" N, 101°27'36.22" E). The aerial imageries of the *Paulownia* tree were taken using Phantom 4 Pro v2.0 (SZ DJI Technology Co., Ltd., China) drone. The camera on the Phantom 4 Pro V2 has a 20-megapixel sensor, an ISO range of 100 to 12800, and is capable of shooting single shots, bursts, auto exposure bracketing, exposure value (EV) bias, and time-lapse. It is equipped with a 1-inch complementary metal oxide semiconductor (CMOS) containing 20 M effective pixels.

It is noteworthy to mention that the number of trees in the study areas varied across different age groups of *Paulownia* trees where there are 929 trees for 3 months old, 1022 trees for 6 months old, 843 trees for 9 months old and 916 trees for 12 months old. These tree counts are summarized in Table 1.

Table 1. Number of *Paulownia* trees at different age groups.

Location	Age (months)	Number of trees
Bahau	3	929
Kundor	6	1022
Kundor	9	843
Rawang	12	916

2.2 Software and hardware

This study employed a template matching technique provided by the Scikit-image Python package. The Scikit-image package was established within the Anaconda Individual Edition software, utilizing Python 3.9 as the programming framework. The process of executing the model in this study was performed by a Lenovo Ideapad Gaming 3 laptop with a central processing unit (CPU) of AMD Ryzen 5 - 5600H powered by a graphic card Nvidia Geforce GTX 1650. Other than that, the random-access memory (RAM) used was 8GB DDR4 3200 MHz.

2.3 Tree counting model

The proposed tree counting algorithm's overall workflow is depicted in Figure 1. Firstly, the image acquisition process was carried out at the Paulownia plantation in the morning, with the time taken for the acquisition spanning from 11:00 AM to 2:00 PM, ensuring clear visibility without fog or cloudy conditions. Secondly, the image undergoes preprocessing method which involves the region of interest selection. The study focused on Paulownia trees categorized into four distinct age groups: 3 months, 6 months, 9 months, and 12 months old. Within each of these groups, a set of 10 images was systematically collected. The cumulative counts of Paulownia trees for each age group were as follows: the 3-month-old

category comprised a total of 929 trees, with an average of 93 trees/image, ranging from 46 to 139 trees; the 6month-old group encompassed 1022 trees in total, yielding an average of 10 trees/image, with a range spanning from 33 to 235 trees; for the 9-month-old group, the total count stood at 843 trees, with an average of 90 trees/image, and a range varying from 51 to 141 trees; finally, the 12-month-old group encompassed 916 trees in total, with an average of 92 trees/image, ranging from 55 to 156 trees. The respective standard deviations for these number of trees at 3, 6, 9 and 12 months were approximately 27.32, 57.74, 24.08, and 29.69. After that, 12 to 15 random points were selected on the image that has been assigned to the region of interest. The image was then converted into a shapefile image containing the reference point for the template selection. The UAVcaptured images were processed to generate image templates, which were subsequently employed for further analysis. Upon processing, the images were incorporated into the analytical framework, and from there, templates of varying sizes were selected. These size categories encompass extra small, small, medium, large, and extra-large.

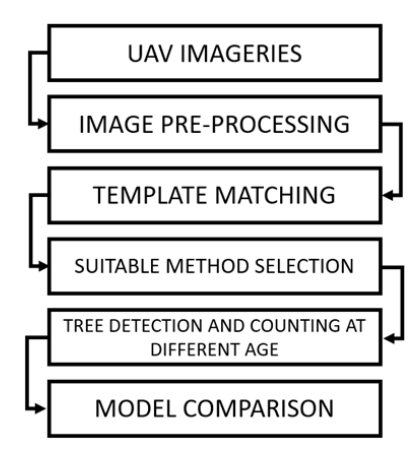


Figure 1. Flowchart of the overall process.

In terms of determining the template sizes, this was achieved through visual assessment and manual cropping. The chosen dimensions were based on the observable characteristics of the trees and their relative sizes. The dimensions of the templates were defined according to the pixel measurements specified in Table 2. These dimensions were selected by considering the relative sizes of the trees, with smaller trees corresponding to smaller template dimensions. These templates were then evaluated for their ability to predict the location of additional trees, and the optimized template was then selected and stored for further analysis. Following the preparation of the optimized template, a template-matching algorithm was used to generate a correlation image. Each pixel in this image represents the correlation coefficient between the template and the subset image of the original image. Following that, a suitable method of template matching

was selected to get a better result. The development of tree counting and detection models for distinct age categories, specifically 3, 6, 9, and 12 months old, relied upon the utilization of the 10-image datasets. The chosen sample size is deemed appropriate for model development based on its capacity to effectively encapsulate the diversity within each tree age group present in the dataset.

Table 2. Template dimensions are based on the number of pixels.

Template size	Dimensions (pixels)
Extra small	23×22
Small	35×40
Medium	41×42
Large	68×62
Extra large	78×73

Additionally, the relationship between size and tree age was examined. It was observed that tree dimensions undergo discernible alterations as they progress through different age stages. Younger trees, such as those at 3 months old, generally manifest smaller sizes that align with the extra small and small template categories. As trees mature to 6 and 9 months, their dimensions tend to increase, often corresponding to the medium and large template categories. Upon reaching the age of 12 months, trees may attain their maximum sizes, characterized by the extra-large template category. This observed correlation between tree age and size served as a guiding principle in the selection of template dimensions, facilitating accurate tree counting and detection. The performance of each model was analyzed and the comparison of which model has the best fit for tree counting at a specific age was obtained.

2.3.1 Image pre-processing

Numerous image pre-processing steps have been performed before detailed analysis. First, the UAV images were visually inspected to ensure that only the highest-quality images were retained. Then, the region of interest was selected in the original UAV imageries to generate ten image datasets in each Paulownia tree age as shown in Figure 2. The size of the region of interest will differ according to the number of Paulownia tree samples contained in the region of interest. The size for the region of interest will be bigger if there are more Paulownia tree samples and will be smaller if there are only a few Paulownia tree samples in a region of interest. After that, the image with the region of interest was then imported to QGIS software to generate the shapefile. Several random points within the range of 12 to 15 were chosen to serve as reference points for generating data on the image. These points were specifically selected to indicate the sampling locations of the regions of interest, which in this case are the *Paulownia* trees. The purpose of these points is to facilitate the creation of templates. The visualization of selecting random points to generate a template image is shown in Figure 3. This step is necessary because reference point data that was stored in shapefile form is needed to generate a template which later will be used in the template matching process.

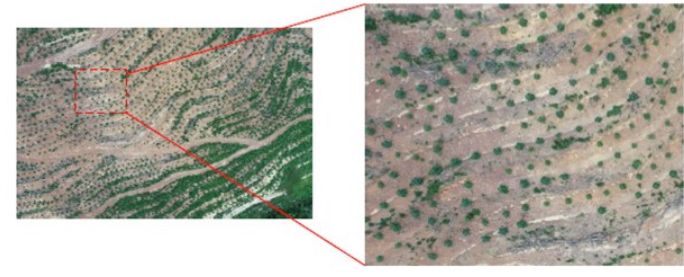


Figure 2. Selecting a region of interest to generate an image dataset.

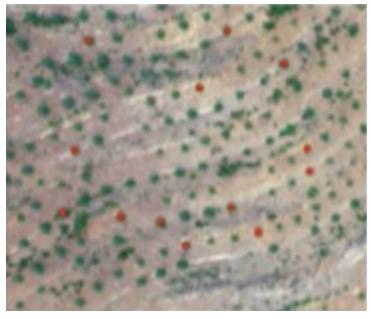


Figure 3. Selecting random points on a region of interest to generate a template image with georeferencing data.

2.3.2 Comprehensive analysis of template generation and matching approaches

This section presents two distinct methods of template generation. The discussion that follows explores these two approaches while also providing an overview of template matching using the generated templates.

2.3.2.1 Template generation process: predetermined size selection from original Paulownia tree image

In order to prepare the image template, different-sized image templates were generated from the original *Paulownia* tree image through a process of visual observation and manual cropping. The sizes were selected based on visually observing the different parts of the original image. Smaller sections were designated as "extra small" templates, followed by slightly larger sections for "small," "medium," "large," and "extralarge" templates, as visualized in Figure 4.

2.3.2.2 Template generation process: Geospatial workflow utilizing geopandas, georeferencing, and raster data

Using the Geopandas library, the image of an aerial view for *Paulownia* (raster data) and the shapefile for the

determined point on the image were imported into the Jupyter Notebook. The shapefile was then generated using a QGIS to georeference the data. Georeferencing is the assignment of locations to geographical objects using a geographic frame of reference. It is essential to geospatial technologies and GIS in general. The output of the georeferencing-processed image was then generated using Jupyter Notebook code. The program only selects the green band using this method. After assigning the code to only search for the green band, the code then executed the point that has been generated in the shapefile to display the number of selected points in the raster data. Visualization for the display is shown in Figure 5. The number of selected points corresponds to the number of template images that will be generated.

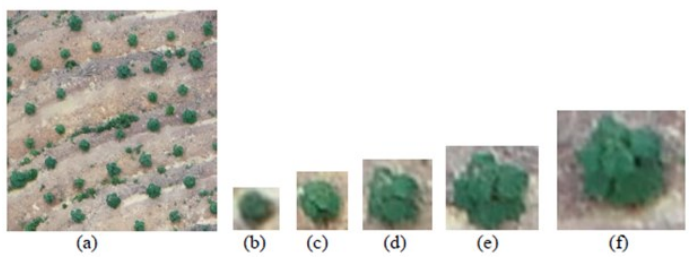


Figure 4. Different template image generated from (a) Original image by using (b) extra small (c) small (d) medium (e) large (f) extra-large.

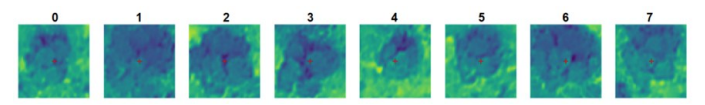


Figure 5. Generated template image according to the selected reference point.

2.3.2.3 Template matching overview and comparative analysis

In this section, an overview of the template matching process is presented robust analytical method. Template matching entails aligning a predetermined template with various sections of an image, aiming to identify regions closely resembling the template. Within the realm of template matching, normalized cross-correlation stands as a common technique.

Normalized cross-correlation serves to quantify the similarity between the template and the image by assessing how effectively the template aligns with diverse image areas. The formula for normalized cross-correlation is as follows:

$$\gamma(u,v) = \frac{\sum_{x,y} \left[f(x,y) - \frac{f}{u,v} \right] [t(x-u,y-v) - \underline{t}]}{\{\sum_{x,y} \left[f(x,y) - \frac{f}{u,v} \right]^2 \sum_{x,y} [t(x-u,y-v) - \underline{t}]^2 \}}$$
(1)

where f is the image, t is the mean of template, and $f_{u,v}$ is the mean of f(x,y) in the region under the template.

By applying normalized cross-correlation to the generated templates, insights can be extracted into the

differences between the two template generation methods and their effectiveness in capturing similar features within the *Paulownia* images.

2.4 Performance model evaluation

Assessing the classification performance of each template-matching approach using different data sources will serve as a benchmark for determining which approach yields the most favourable outcomes. In this study, a confusion matrix was used to quantify the performance of a classification algorithm. It visualizes and summarizes a classification algorithm's performance. The confusion matrix is composed of four fundamental characteristics (numbers) that are used to define the classifier's measurement metrics. True Positive (TP) represents the number of correctly identified Paulownia trees. True Negative (TN) indicates the number of correctly classified as other than Paulownia. False Positive (FP) indicates a pixel that appears to be a Paulownia tree but is something else. Additionally, FP is referred to as a Type I error. False Negative (FN) indicates that no Paulownia tree was detected. The FN error is also referred to as a Type II error. The accuracy, precision, recall, and F1-score of an algorithm are calculated using the TP, TN, FP, and FN.

The accuracy of an algorithm is expressed as the ratio of correctly classified *Paulownia* trees (TP+TN) to all *Paulownia* trees (TP+TN+FP+FN), calculated as in Equation (2).

$$Accuracy = \frac{(TP + TN)}{(TP + FP + TN + FN)}$$
 (2)

Precision can be thought of in this sense as the chance of detecting a legitimate *Paulownia* tree, calculated as in Equation (3).

$$Precision = \frac{TP}{TP + FP}$$
 (3)

The probability of detecting the correct *Paulownia* tree (ground truth) is called recall, calculated as in Equation (4).

$$Recall = \frac{TP}{TP + FN} \tag{4}$$

F1 is also referred to as the F Measure. The F1 score is the balance of precision and recall, calculated as in Equation (5).

F1 score =
$$\frac{2 * \text{precision} * \text{recall}}{\text{precision} + \text{recall}}$$
 (5)

3. Results and discussion

3.1 Template matching selection

Figure 6 shows the result of template matching using

the predetermined size of the template image and template matching using geo-referencing data. Both methods can detect 32 out of 40 *Paulownia* trees in the image. The sizes of template images were generated by adjusting the threshold for each template image size. As a result, a threshold value of 0.7 was chosen for extrasmall image templates, 0.75 for small, 0.80 for medium, 0.85 for large, and 0.90 for extra-large images. As shown in Figure 6a, the method performed well in detecting extra small, small, medium and large trees where the detected points were overlapping with the tree's canopy. However, when detecting the extra-large trees, the detect points did not give accurate positions.

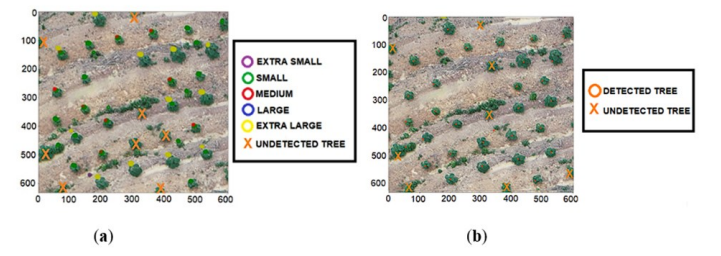


Figure 6. Results of template matching (a) Template matching according to the predetermined size of template image and (b) Template matching with georeferencing data.

As shown in Figure 6b, template matching using georeferencing data demonstrated more accurate results where the detected points were overlapping with the tree's canopy. This method not only could detect the trees but also provide the exact location of the trees. However, this method did not provide information about the size of the canopy. Since the main aim of this study is to detect and count the number of *Paulownia* trees, therefore the canopy classification is not a priority. Other than that, the template matching by using specific sizes used different sizes of templates to detect specific results of tree size in a dataset. If the size of the tree in the dataset is bigger or smaller than the predetermined size of the template, thus it will not detect the tree.

As a result, template matching with georeferencing data was chosen over template matching according to the predetermined size of the template image because it not only demonstrates more accurate results but is also more convenient for the user to count the tree with fewer processing steps. Moreover, this method could determine the exact location of the tree because it represents the actual coordinates of the tree on a specific latitude and longitude. Even though template matching according to the predetermined size of the template image could provide information about canopy size, however, it requires a long processing stage where the user needs to acquire several cropped template images from the original image with different sizes which were extra small, small, medium, large, and extra-large.

3.2 Paulownia tree detection and counting

This section presents the results of tree counting detected using a template matching with georeferencing data. Moreover, this section presents the results of *Paulownia* tree detection and counting using a model developed using the tree's respective age. *Paulownia* tree counting and detection at a specific age such as 3, 6, 9 and 12 months old was done to obtain results of which model was suitable to be used for tree detection and counting.

3.2.1 Paulownia tree detection and counting at 3 months old

Table 3 shows the model performance obtained from ten different image datasets for the 3-month-old *Paulownia* trees represented by its value of accuracy, precision, recall, and F1-score. In general, based on the average score, the model demonstrated good performance in detecting the *Paulownia* tree with an acceptable value of accuracy (76.05%), precision (86.97%), recall (86.88%) and F1-score (86.21%). The overall performance shows that the F1-score is between 78.9% to 92.5%

3.2.2 Paulownia tree detection and counting at 6 months old

Table 4 shows the detailed results of the *Paulownia* tree detection and counting model at 6 months old obtained from ten different image datasets. The average score of the accuracy, precision, recall and F1-score were 74.8%, 89%, 82.38% and 85.45%, respectively. As stated in Table 2, image dataset 9 has the highest accuracy with 81.96% compared to the lowest accuracy of 66.15% in dataset 3. For precision, based on Table 2, dataset 10 shows the highest value with 98.3% while dataset 3 gave the lowest precision value with only 78.1%. For recall, the highest value is 88.79% obtained from dataset 1 while the lowest recall value is in dataset 4 with only 74.04%. Lastly, for the F1-score, the highest value is 90.09% in dataset number 9 while the lowest is 79.62% which is in dataset 3.

3.2.3 Paulownia tree detection and counting at 9 months old

Table 5 provides results for ten distinct image datasets utilizing a 9-month-old *Paulownia* tree. According to Table 3, the average value performance parameters which were the accuracy, precision, recall and F1-score were 73.95%, 91.73%, 79.31% and 84.95%, respectively. Dataset 5 has the highest accuracy at 79.31%, while dataset 2 has the lowest accuracy at 64.47%. Moreover, dataset 5 also has the highest precision with 97.87 %, whereas dataset 9 has the lowest

Table 3. Model performance for 3-month-old *Paulownia* trees image datasets.

Dataset	A atual	TD	ED	ENI	Accuracy	Precision	Recall	F1-score
no	Actual	TP	FP	FN	(%)	(%)	(%)	(%)
1	46	39	4	7	78.00	90.70	84.78	87.64
2	86	58	3	28	65.17	95.08	67.44	78.91
3	77	59	2	18	74.68	96.72	76.62	85.51
4	60	57	23	3	68.67	71.25	95.00	81.43
5	139	124	32	15	72.51	79.49	89.21	84.07
6	115	105	7	10	86.07	93.75	91.30	92.51
7	112	98	4	14	84.48	96.08	87.50	91.59
8	94	90	11	4	85.71	89.11	95.74	92.31
9	80	71	13	9	76.34	84.52	88.75	86.59
10	120	111	41	9	68.94	73.03	92.50	81.62
	Average					86.97	86.89	86.22

Table 4. Model performance for 6-month-old *Paulownia* trees image datasets.

Dataset	A 4 1	TD	ED	EM	Accuracy	Precision	Recall	F1-score
no	Actual	TP	FP	FN	(%)	(%)	(%)	(%)
1	116	103	15	13	78.63	87.29	88.79	88.03
2	113	96	5	17	81.36	95.05	84.96	89.72
3	53	43	12	10	66.15	78.18	81.13	79.63
4	235	174	22	61	67.70	88.78	74.04	80.74
5	105	86	19	19	69.35	81.90	81.90	81.90
6	123	99	19	24	69.72	83.90	80.49	82.16
7	33	28	2	5	80.00	93.33	84.85	88.89
8	40	32	4	8	72.73	88.89	80.00	84.21
9	58	50	3	8	81.97	94.34	86.21	90.09
10	146	119	2	27	80.41	98.35	81.51	89.14
	Average					89.00	82.39	85.45

Table 5. Model performance for 9-month-old *Paulownia* trees image datasets.

-	1							
Dataset	Actual	TP	FP	FN	Accuracy	Precision	Recall	F1-score
no	Actual	ctuai IP	гР	ΓIN	(%)	(%)	(%)	(%)
1	93	76	5	17	77.55	93.83	81.72	87.36
2	67	49	9	18	64.47	84.48	73.13	78.40
3	141	113	17	28	71.52	86.92	80.14	83.39
4	79	59	2	20	72.84	96.72	74.68	84.29
5	114	92	2	22	79.31	97.87	80.70	88.46
6	83	69	5	14	78.41	93.24	83.13	87.90
7	75	58	4	17	73.42	93.55	77.33	84.67
8	103	83	2	20	79.05	97.65	80.58	88.30
9	88	75	16	13	72.12	82.42	85.23	83.80
10	51	39	4	12	70.91	90.70	76.47	82.98
		Average			73.96	91.74	79.31	84.95

Table 6. Model performance for 12-month-old Paulownia trees image datasets.

Dataset	Actual	TP	FP	FN	Accuracy	Precision	Recall	F1-score
no	Actual	11	г٢	riN	(%)	(%)	(%)	(%)
1	80	51	7	29	58.62	87.93	63.75	73.91
2	62	50	0	12	80.65	100.00	80.65	89.29
3	76	60	8	16	71.43	88.24	78.95	83.33
4	156	123	9	33	74.55	93.18	78.85	85.42
5	107	84	23	23	64.62	78.50	78.50	78.50
6	89	68	2	21	74.73	97.14	76.40	85.53
7	131	95	7	36	68.84	93.14	72.52	81.55
8	55	39	4	16	66.10	90.70	70.91	79.59
9	78	51	8	27	59.30	86.44	65.38	74.45
10	82	61	4	21	70.93	93.85	74.39	82.99
		Average			68.98	90.91	74.03	81.46

precision with 82.41%. The highest recall was obtained from dataset 9, with a value of 85.22%, while the lowest recall was obtained from dataset 2, with only 73.13%. Meanwhile, the highest F1-score is 88.46%, obtained from dataset 5, while the lowest is 78.4%, obtained from dataset 2.

3.2.4 Paulownia tree detection and counting at 12 months old

Table 6 tabulates the various performance parameters including accuracy, precision, recall, and F1score, based on ten distinct image datasets for 12-monthold Paulownia trees. The average score of the accuracy, precision, recall and F1-score were 73.96%, 91.74%, 79.31% and 84.95%, respectively. Dataset 2 has been identified as the dataset with the highest accuracy with 80.64%, while dataset 1 obtained the lowest accuracy, with 58.62 %. Meanwhile, dataset 2 obtained 100% precision. Dataset 5 obtained the lowest precision, with a value of 78.50%. The dataset with the highest recall is dataset 2, with 80.64%, while the dataset with the lowest recall is dataset 1, with 63.75%. Dataset 5 also obtained the highest F1-score, with a value of 89.28 %. The dataset with the lowest F1-score is dataset 1, with 73.91%.

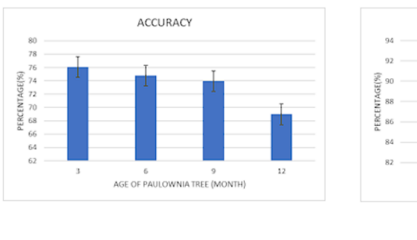
3.3 Performance comparison at different growing stages

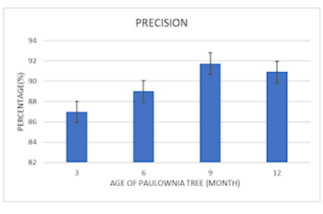
As shown in Figure 7, in general, the model performance reduced as the age of the tree increased. For example, in accuracy (Figure 7a), *Paulownia* trees at 3 months old had the highest percentage of accuracy with a value of 76.05%. It is then followed by 6 months old (74.80%), 9 months old (73.95%) and 12 months old (68.97%). One of the factors of the highest average percentage is due to the model can easily differentiate the *Paulownia* tree from other elements in the dataset. Meanwhile, the dataset with 12 months old *Paulownia* trees has the lowest average percentage of accuracy. This is because, in the dataset of 12 months old *Paulownia* tree model, the crowns were overlapping with each other thus making it difficult to detect *Paulownia* trees.

For precision, a different trend was observed as shown in Figure 7b. In general, the percentage score of precision was increased from 3 to 6 to 9 months old, but a little bit dropped at 12 months old. The 9-month-old detection models obtained the highest precision score with 91.73%, then followed by 12-month-old (90.91%), 6-month-old (89.0%) and finally 3-month-old (86.97%). It shows that the 9-month-old model has more confidence when it classifies a sample as positive compared to the other models, in this case, the model has more confidence in detecting a true *Paulownia* tree. For 3-month-old model, has the lowest average for precision

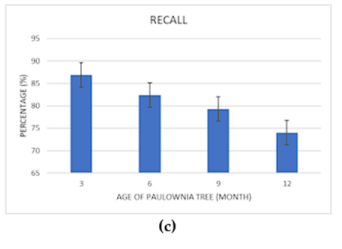
due to the classifier returning a lot of false positives.

For recall (Figure 7c), the highest average percentage for recall is 3-month-old with 86.88%, followed by 6-month-old (82.38%), 9 months old (79.31%) and 12 months old (74.03%). For the 3-month-old model, it has the highest percentage for recall due to the algorithm returns most of the relevant results. Other than that, the 3-month-old model also returns more results as well as the predicted number of *Paulownia* trees is correct compared to the actual number of *Paulownia* trees. Next, the model for the 12-month-old *Paulownia* tree has the lowest average percentage for recall due to most of the positive values, in this case, the true *Paulownia* trees were never predicted or detected.





(b)



(a)

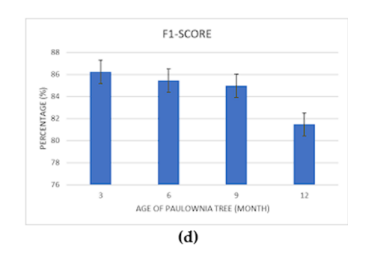


Figure 7. Comparison graph of model performance score based on (a) accuracy (b) precision (c) recall and (d) F1-score at different *Paulownia* tree ages.

For F1-score (Figure 7d), the highest average value was obtained from 3 months old with 86.21%, then followed by 6 months old (85.45%), 9 months old (84.95%) and finally 3 months old (81.45%). *Paulownia* tree model with 3 months old age has the highest average percentage for F1-score. The closest the value of F1-score to 100% means that the better the model is compared to the other model and vice versa. For 12-month-old model, has the lowest average percentage of F1-score among the 4 models of *Paulownia*'s tree age. In this case, the 12-month-old model has the lowest performance when classifying any observation into the correct class.

Based on all of the confusion matrix parameters that have been used to compare the performance between the tree detection and counting model at different growing stages, it can be seen that younger *Paulownia* such as 3 and 6 months old are performing well in terms of accuracy and F1-score, which meant the model can

identify the correct classification as *Paulownia* tree. The presence of shadows from neighbouring bushes, as well as the colour resemblance of the bushes with the trees, resulted in a lower performance. This happened in the oil palm application studied by Hanapi *et al.* (2021) as well.

4. Conclusion

This study has demonstrated that template matching with georeferencing data was more reliable than template matching using the predetermined size of the template image since it can accurately detect the location of the Paulownia tree. Moreover, based on this study, it is also shown that template matching with georeferencing data needs to be developed according to the specific ages such as 3, 6, 9 and 12 months old due to Paulownia tree phenotypes during plant growth which is more related with the architecture parameters. Other than that, based on this study, the overall model performance of younger Paulownia tree ages i.e., 3 and 6 months old performs the best where both of the models has F-1 score of more than 85%. This is due to the younger Paulownia tree having a smaller tree crown thus it does not overlap with each other making the algorithm easily detect the similar tree crown based on the image template that has been assigned. This observation is substantiated by the fact that young Paulownia trees display a higher level of uniformity in their crown shape and exhibit more distinct separation between individual crowns compared to mature Paulownia trees, which often have crowns that overlap with each other.

To improve the overall performance of the model in future work, we can enhance the raw images by applying preprocessing techniques before importing them into the Jupyter Notebook database for template matching. Therefore, additional research should be conducted to develop tree detection and counting with template matching by differentiating the crown shape of *Paulownia* from the soil surface. Other than that, the *Paulownia* tree detection and counting research can be further enhanced by defining the weeds as the unwanted object to be recognized in the programming command. This will make it easier for the algorithm to detect only trees during the process of template matching.

Conflict of interest

The authors declare no conflict of interest.

Acknowledgements

The authors would like to acknowledge Green Afforestation International Network Sdn. Bhd for providing the datasets.

References

- El-Showk S. and El-Showk N. (2003). The *Paulownia* Tree. An Alternative for Sustainable Forestry, *Crop Development*. Retrieved August 6, 2022, from website: http://www.cropdevelopment.org/docs/*Paulownia*Brochure print.pdf
- Gomes, M.F. and Maillard, P. (2013). Identification of urban tree crown in a tropical environment using WorldView-2 data: problems and perspectives. *Proceedings of the 2013 SPIE Remote Sensing*, 8893, 60-72. https://doi.org/10.1117/12.2029073
- Hanapi, S.N.H.S., Shukor, S.A.A. and Johari, J. (2021).

 Normalized Cross Correlation Template Matching for Oil Palm Tree Counting from UAV image. *Journal of Physics: Conference Series*, 2107(1), 012036. https://doi.org/10.1088/1742-6596/2107/1/012036
- Hung, C., Bryson, M. and Sukkarieh, S. (2012) Multi-Class Predictive Template for Tree Crown Detection. *ISPRS Journal of Photogrammetry and Remote Sensing*, 68, 170-183. https://doi.org/10.1016/j.isprsjprs.2012.01.009
- Kaygin, B., Kaplan, D. and Aydemir, D. (2015). *Paulownia* tree as an alternative raw material for pencil manufacturing. *BioResources*, 10(2), 3426-3433. https://doi.org/10.15376/BIORES.10.2.3426-3433
- Kertész, G., Szénási, S. and Vámossy, Z. (2015). Performance measurement of a general multi-scale template matching method. *IEEE 19th International Conference on Intelligent Engineering Systems*, 2015, 153-157. https://doi.org/10.1109/INES.2015.7329697
- Koman, S., Feher, S., and Vityi, A. (2017). Physical and Mechanical Properties of *Paulownia tomentosa* Wood Planted in Hungary. Retrieved on September 8, 2024, from Wood Research website: http://www.woodresearch.sk/wr/201702/15.pdf
- Krikorian, A.D. (1988). *Paulownia* in China: Cultivation and Utilization. *Economic Botany*, 42(3), 451-451. https://doi.org/10.1007/BF02860168
- Latib, H.A., Liat, L.C., Ratnasingam, J., Law, E.L., Aziin, A.A.A., Mariapan, M. and Natkuncaran, J. (2020). Suitability of *Paulownia* wood from Malaysia for furniture application. *BioResources*, 15 (3), 4727-4737. https://doi.org/10.15376/biores.15.3.4727-4737
- Larsen, M. and Rudemo, M. (1998). Optimizing templates for finding trees in aerial photographs. *Pattern Recognition Letters*, 19(12), 1153-1162. https://doi.org/10.1016/S0167-8655(98)00092-0
- Larsen, M., Eriksson, M., Descombes, X., Perrin, G.,

- T. and Brandberg, Gougeon, F.A. (2011).Comparison of six individual tree crown detection algorithms evaluated under varying forest conditions. International Journal of Remote Sensing, 32(20),5827-5852. https:// doi.org/10.1080/01431161.2010.507790
- Maillard, P. and Gomes, M.F. (2016). Detection and counting of orchard trees from VHR images using a geometrical-optical model and marked template matching. *ISPRS Annals of the Photogrammetry, Remote Sensing and Spatial Information Sciences*, 3, 75-82. https://doi.org/10.5194/ISPRS-ANNALS-III-7-75-2016
- Olofsson, K., Wallerman, J., Holmgren, J. and Olsson, H. (2006). Tree species discrimination using Z/I DMC imagery and template matching of single trees. *Scandinavian Journal of Forest Research*, 21(S7), 106-110. https://doi.org/10.1080/14004080500486955
- Pollock, R. (1996). The automatic recognition of individual trees in aerial images of forests based on a synthetic tree crown image model. Canada: University of British Columbia, Ph.D. Thesis.
- Pouliot, D.A., King, D.J., Bell, F.W. and Pitt, D.G. (2002). Automated tree crown detection and delineation in high-resolution digital camera imagery of coniferous forest regeneration. *Remote Sensing of Environment*, 82(2-3), 322-334. https://doi.org/10.1016/S0034-4257(02)00050-0
- Quackenbush, L., Hopkins, P.F. and Kinn, G.J. (2000). Developing forestry products from high resolution digital aerial imagery. *Photogrammetric Engineering and Remote Sensing*, 66, 1337-1346.
- Vahidi, H., Klinkenberg, B., Johnson, B.A., Moskal, L.M. and Yan, W. (2018). Mapping the individual trees in urban orchards by incorporating Volunteered Geographic Information and very high resolution optical remotely sensed data: A template matching-based approach. *Remote Sensing*, 10(7), 1134. https://doi.org/10.3390/rs10071134
- Wagner, F.H., Ferreira, M.P., Sanchez, A., Hirye, M.C.M., Zortea, M., Gloor, E., Phillips, O.L., de Souza Filho, C.R., Shimabukuro, Y.E. and Aragão, L.E.O.C. (2018). Individual tree crown delineation in a highly diverse tropical forest using very high resolution satellite images. *ISPRS Journal of Photogrammetry and Remote Sensing*, 145(Part B), 362-377. https://doi.org/10.1016/J.ISPRSJPRS.2018.09.013
- Wang, Y., Zhu, X. and Wu, B. (2018). Automatic detection of individual oil palm trees from UAV images using HOG features and an SVM classifier. *International Journal of Remote Sensing*, 40(19),

- 7356-7370. https://doi.org/10.1080/01431161.2018.1513669
- Xie, Y., Bao, H., Shekhar, S. and Knight, J. (2018). A TIMBER Framework for Mining Urban Tree Inventories Using Remote Sensing Datasets. 2018 IEEE International Conference on Data Mining, 2018, 1344-1349. https://doi.org/10.1109/ICDM.2018.00183
- Zainuddin, N.E. and Daliman, S. (2020). Analysis of Rubber Tree Recognition Based on Drone Images. *IOP Conference Series: Earth and Environmental Science*, 549(1),012012. https://doi.org/10.1088/1755-1315/549/1/012012